ORIGINAL PAPER

Colorimetric determination of cysteine by a paper-based assay system using aspartic acid modified gold nanoparticles

Chunye Liu[1] · Yanqing Miao[1] · Xuejiao Zhang[1] · Shuli Zhang[2] · Xiaojun Zhao[1]

Abstract

A method is described for cysteine (Cys) determination on paper-based analytical devices using aspartic acid modified gold nanoparticles (Asp-AuNPs). The Asp-AuNPs were characterized by their size, zeta potential, and UV-visible absorption spectrum. After the addition of Cys, it will interact with Asp-AuNPs selectively and leads to the aggregation of Asp-AuNPs. A color change from red to blue can be observed on the paper-based analytical devices. The results were recorded using a cell phone and subsequently analyzed using the Photoshop software. The ratiometric color intensity at red channel and blue channel (Red/Blue) increased linearly in the range 99.9–998.7 μM for Cys ($R = 0.9984$), and the limit of detection was 1.0 μM. The effects of assay conditions have been investigated and are discussed. The Cys concentration was determined as $(0.27 \pm 0.02$ mM) in human plasma, and the recovery was from 99.2 to 101.1%.

Keywords Gold nanoparticles · Microfluidic paper-based analytical devices · Cysteine · Colorimetric assay · Aspartic acid · Ratiometric color intensity

Introduction

Small molecules of biothiols are closely related to the occurrence and development of various diseases [1–3]. For example, abnormal levels of cysteine (Cys) can result in slow growth, skin lesions, lethargy, liver damage, severe neurotoxicity, and cardiovascular diseases [4–6]. Therefore, the determination of Cys in a physiological system is of great significance to early clinical diagnosis of the above diseases. In general, several methods [7–18] have been applied for biothiols quantitation such as high-performance liquid chromatography (HPLC) [7], capillary electrophoresis [8], and fluorescence method [10].

As a point-of-care testing system, microfluidic paper-based analytical devices (μPADs) provide a promising platform for biochemical assays with the advantages of low cost, portability, and disposability [19–28]. μPADs are usually integrated with colorimetric systems because of its simplicity. As the nanoparticles can change their color depending on their shape, size, and distance between the particles, they have been widely employed in colorimetric determination [25, 29–36]. Some reported nanomaterial-based colorimetric determinations for Cys were listed in Table 1. However, the surrounding conditions in the solution can affect the aggregation or disaggregation of the particles. To overcome the limitation, Prasetia et al. formed nanoparticles on a hydroxyapatite solid support [36]. To the best of our knowledge, few studies on nanoparticles for quantification of Cys on μPADs using colorimetric system have been reported to date.

Aspartic acid (Asp) modified gold nanoparticles (Asp-AuNPs) were synthesized and used as a colorimetric indicator. Using the Asp-AuNPs, Cys was determined on paper-based devices via a simple ratiometric color intensity method. Different from general colorimetric determination, the results were recorded using a cell phone. The color intensity was obtained by the Photoshop software. A ratiometric color intensity method was designed for the analysis. The effects of assay conditions were investigated systemically. Cys

✉ Chunye Liu
doris8976@163.com

1   School of Pharmacy, Xi' an Medical University, Xi'an 710021, China

2   Department of Medical Technology, Xi' an Medical University, Xi'an 710021, China

Table 1 An overview on recently reported nanomaterial-based optical determination of Cys

Material	Method	Merits	Reference
Gold nanoparticles (AuNPs) and aspartic acid (1.8 mM) solution	Visualized with the naked eye and determined by UV–vis spectroscopy	Linear range was from 0.166 to 1.67 μM, and the limit of detection (LOD) is 100 nM. Higher selectivity and anti-interference.	[29]
Silicon quantum dots (SiQDs) modified AuNPs	Colorimetric and fluorescence detection (with excitation/emission peaks at 430/520 nm)	Lower LOD (3.5 nM), and the method works on the 0.01–2 μM Cys concentration range.	[30]
Flower extract of *Acmella oleracea* modified AuNPs	UV–vis spectroscopy and LSPR-based fiber optic detection	Has a wide linear range (50–1000 μM). The LOD was 0.0779 μM.	[32]
Chitosan stabilized AuNPs	UV–vis spectroscopy	Simple and high selectivity. LOD was 0.1 μM and the linear range was from 0.1 to 30 μM.	[33]
ss DNA-stabilized AuNPs	UV–vis spectroscopy (ratio of absorptions at (A_{640}/A_{525}))	Higher selectivity and low cost. The LOD was 100 nM, the linear range was 0.1–0.5 μM.	[34]
Pd-based enzymatic nanoparticles	UV–vis spectroscopy	Higher selectivity and sensitivity (LOD was 3.7 nM). The linear range was from 10 to 150 nM.	[35]
Silver nanoparticles (AgNPs) on hydroxyapatite (HAp).	Color intensity was measured by Image-J program	The linear range was from 0 to 105 μM, and the LOD was 2.03 μM.	[36]
Aspartic acid modified AuNPs	Results recorded by a cell phone and the color intensity was measured by the Photoshop software. A ratiometric color intensity method was used for the analysis.	Not require apparatus. Simple and high selectivity. The LOD was 1.0 μM. The linear range was from 99.9 to 998.7 μM	This work

concentration of human blood plasma was obtained under the optimum conditions.

Materials and methods

Apparatus and reagents

DL-aspartic acid (98%), DL-cysteine (97%), DL-homocysteine (95%), ascorbic acid (≥ 99%), and chloroauric acid (HAuCl$_4$·3H$_2$O, 99.9%) were all from Shanghai Aladdin Bio-Chem Technology Co., LTD (https://www.aladdin-e.com/, Shanghai, China). Glutathione (≥ 98%) was obtained from TCI (Shanghai) Development Co., LTD (https://www.tcichemicals.com/zh/cn/, Shanghai, China). Trisodium citrate and sodium sulfite were purchased from Tianjin Sheng'ao Chemical Reagent Co., Ltd. (http://5583800.1024sj.com/, Tianjin, China). Chitosan was from Shanghai Hefeng pharmaceutical Co., Ltd. (http://www.shharvest.com/, Shanghai, China). All the reagents were analytical grade unless otherwise stated. Blood plasmas of healthy volunteers were obtained from the Department of Medical Technology, Xi'an Medical University. Deionized water was used in all the experiments. Whatman No. 1 qualitative papers were purchased from Whatman (Maidstone, Kent, http://whatman.utopbio.com/, UK). Nanoparticle size and zeta potential were analyzed with Malvern Zetasizer Nano zen3600 (Malvern Instruments, Worcestershire, http://www.malvern.com/, UK). Huawei 5s cell phone was from Huawei Technologies Co. Ltd. (https://www.huawei.com.cn/, Guangdong, China). Adobe Photoshop CS2 (PS 9.02) was from Adobe Systems Incorporated (California, https://www.adobe.com/, USA).

Experimental procedures

Synthesis of the Asp-AuNPs

The AuNPs were synthesized based on the sodium citrate synthesis method similar as reported previously [29]. The syntheses in adequate detail were given in the Electronic Supporting Material (ESM). Then, 20 μL of 2 mM aspartic acid (Asp) was added into 5 mL above AuNP solution. The solution was stirred for 2 h at room temperature to obtain the Asp-AuNP solution. The obtained Asp-AuNP solution was stored in refrigerator at 4 °C, and filtered with 0.45 μm pore membrane filters prior to use.

Sample preparation

The sample preparation was similar as reported previously [37]. In briefly, acetone (300 μL) was added to 100 μL fresh plasma and centrifuged at 8000 rpm (214.6 g) for 10 min.

Then, the supernatant was dried with N_2 gas and 1000 μL deionized water was added to obtain the plasma sample.

Preparation of paper-based platform

Round-shaped Whatman No. 1 qualitative papers were cut with a hole puncher, each with a diameter of 6 mm. To avoid the rapid leaching of nanoparticles from the paper surface, 6.0 μL of 0.25 mg mL^{-1} chitosan solution was spotted in the paper and dried at room temperature initially. Figure 1a displays the preparation procedure of the paper-based analysis platform.

The performance of the assay

Asp-AuNP solution with volume of 7 μL was dropped on above paper-based platform. They were entrapped onto the surface through the hydrogen bonding between chitosan and Asp. Then, 7 μL analyte was spotted. After action for 2 min, the results were recorded using a Huawei 5s camera under a lamp (LED lamp, 3 W power). The distance between paper-based platform and the light source was 20 cm. These conditions make the same brightness when taking a picture. For multiple sample tests, the analyses were conducted one by one. The experimental
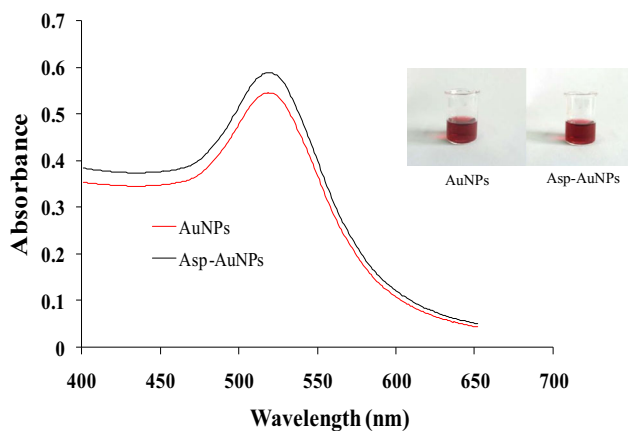
Fig. 2 UV-Vis spectra of AuNPs and Asp-AuNPs. Inset is the photographs of AuNPs and Asp-AuNPs

procedure and ratiometric color intensity method are shown in Fig. 1b.

The ratiometric color intensity method

The images were analyzed using Adobe Photoshop CS2 as follows. First, the images were scanned using the CS scanning application software (IntSig Information Co., Ltd) that was installed on the Huawei 5s. The image is similar to the result of the scanner after CS software processing. Second,
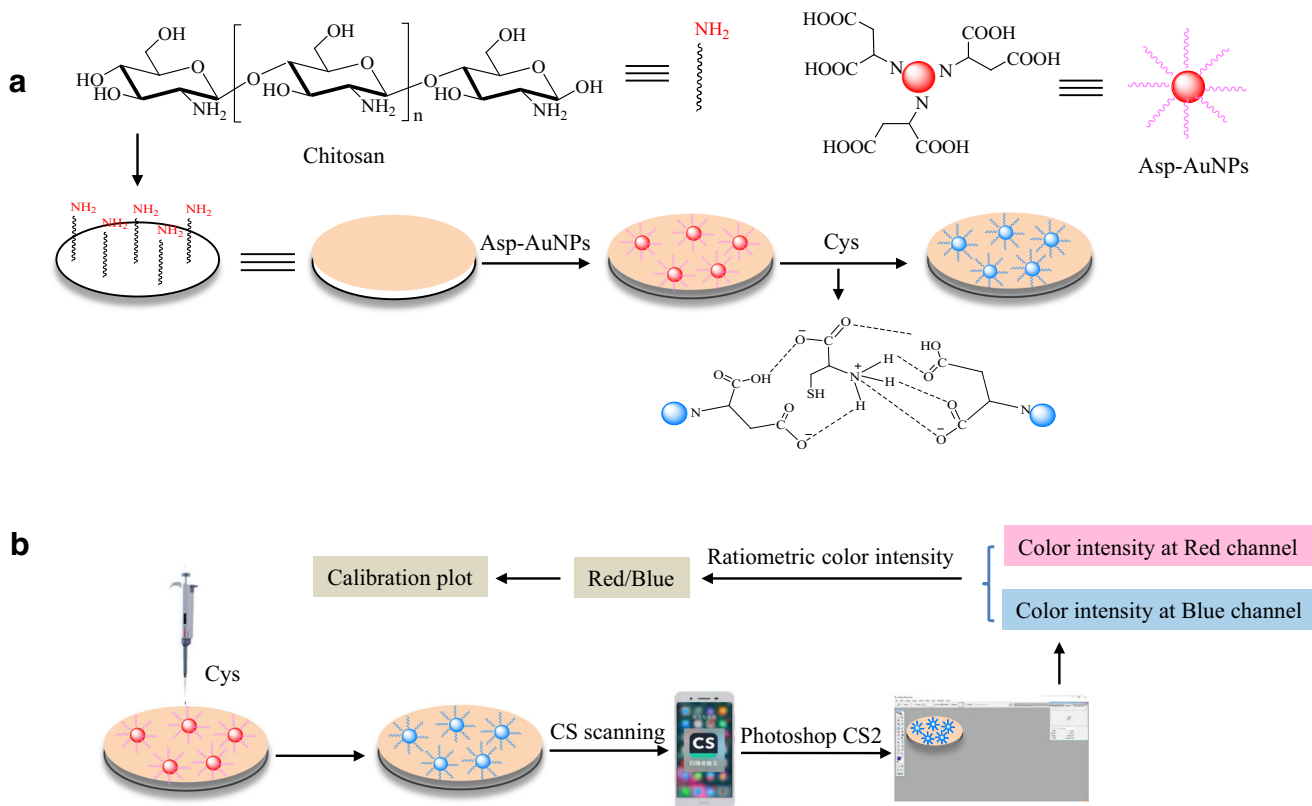
Fig. 1 **a** Preparation of the paper-based analysis platform. **b** Experimental procedure and illustration of the ratiometric color intensity method

Fig. 3 Calibration curve and
LOD of Cys detection. **a**
Calibration curve and
photographs of Cys detection
obtained by Huawei 5s at 2 min. **b**
Photographs of Cys detection at
2 min. Asp-AuNPs and Cys were
fixed at 7 μL and 9 μL,
respectively
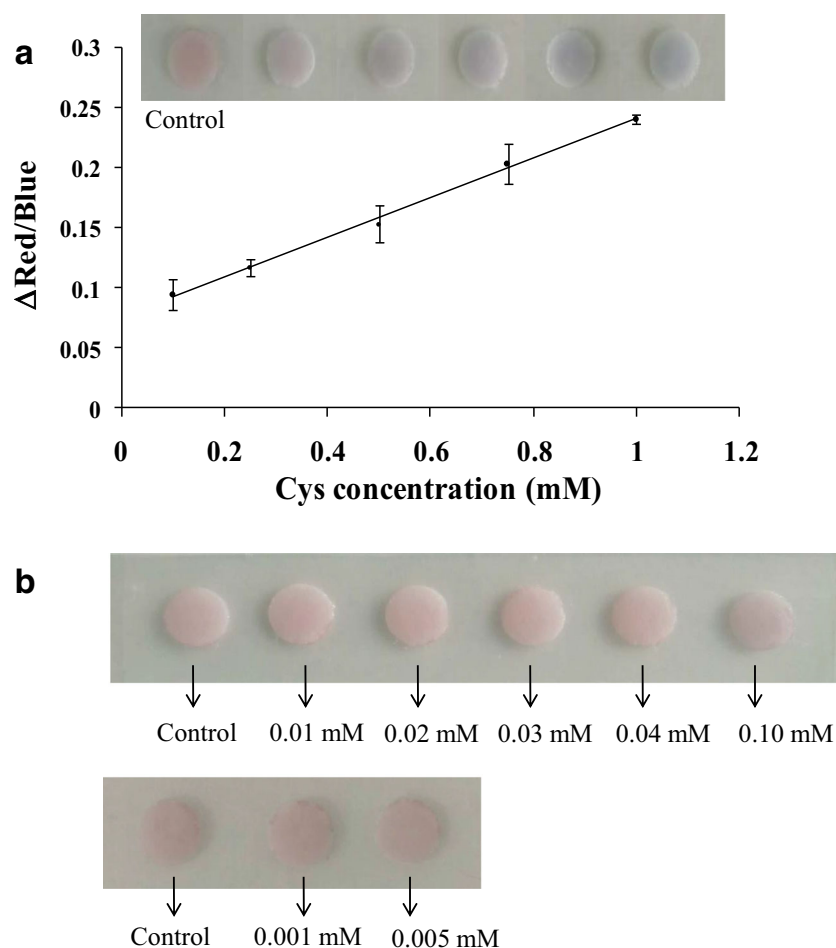
the color intensity was obtained by measuring "mean" value of the corresponding channel with Photoshop CS2. The procedure of Photoshop analysis is as follows. Open "Histogram" in the "Window" menu, and then select "Red" (or "Blue") channel. "Pixels" was chosen as 380. The "mean" intensity is obtained when the keys "control" and "I" were pressed at the same time. At last, the Red/Blue value was calculated by dividing the "mean" value of Red channel to that of Blue channel.

Results and discussion

Principle of the determination

The approach is based on the aggregations of Asp-AuNPs. Resulting from the aggregation of Asp-AuNPs, the color gradually changes from red to blue as the concentration of Cys is increasing. It is attributed to the ion pair interactions between Cys and Asp. The interaction strength is directly related to the molecular structure and the charged groups [29]. Amino group and carboxyl group of Cys can change the intermolecular ion pair interaction of Asp-AuNPs. The higher the concentration of Cys, the faster aggregation and the more obvious color change. According to the results of Adobe Photoshop CS2, the color intensity of "Red" and "Blue" channels was all gradually changing. It is found that the Red/Blue ratio is proportional to the Cys concentration. Therefore, the average Red/Blue ratio was used to quantify the concentration of Cys in the sample.

Table 2 Comparison of the experimental and theoretical results of Cys based on the calibration plot

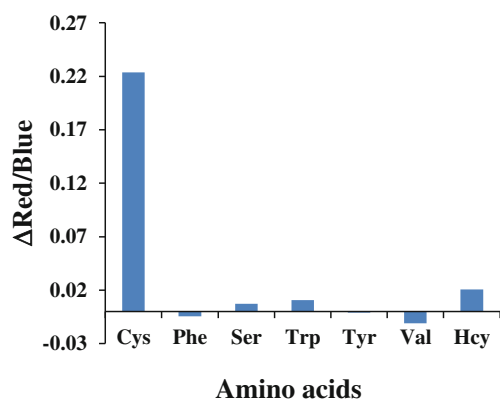| Cys in samples/μg	Added Cys/μg	Found Cys/μg	Recovery/%	Average recovery/%
3.03	1.2	4.25	102.0	98.8
	3.0	5.93	96.5	
	4.0	6.94	97.9	
6.06	3.1	9.31	104.7	98.9
	5.7	11.60	96.9	
	8.3	14.00	95.2	
9.09	4.5	13.80	104.7	102.0
	9.3	18.80	104.8	
	12.3	21.00	96.6	

Fig. 4 Selectivity test of the Cys compared with other amino acids. Asp-AuNPs and amino acids were fixed at 7 μL and 9 μL, respectively. The concentration of amino acids and action time were 0.78 mM and 2 min, respectively

Characterization of Asp-AuNPs

The size and zeta potential of AuNPs and Asp-AuNPs were analyzed on Malvern Zetasizer Nano zen3600 instrument. The particle size of AuNPs and Asp-AuNPs was (37.3 ± 0.1 nm) and (54.4 ± 0.2 nm), respectively. The zeta potential of AuNPs and Asp-AuNPs was (-20.1 ± 1.0 mV) and (-33.3 ± 0.7 mV), respectively. The successful bonding of Asp to AuNPs can be proved by the increased particle size. The dispersion of Asp-AuNPs is stable which may attribute to its higher absolute value of zeta potential.

To confirm the existence of Asp on AuNP surface, UV-visible absorption spectrum was also investigated (Fig. 2). The maximum absorption of Asp-AuNPs is 521 nm. Compared with AuNPs (518 nm), it has a red shift. The color and the maximum absorption of Asp-AuNPs have no obvious changes after 30 days. It shows the good stability of the Asp-AuNPs.

Optimization of method

The following parameters were optimized: (a) the Asp-AuNP volume; (b) the sample (Cys) volume; (c) action time. Respective text and figures on optimizations were given in the ESM. In short, the following experimental conditions were found to give best results: (a) Best volume of Asp-AuNPs was 7 μL; (b) best volume of Cys sample was 9 μL; and (c) best action time was 2 min.

The calibration plot of Cys

To determine the concentration of Cys in samples, a calibration plot was fabricated. First, 7 μL Asp-AuNP was added onto the round paper, and then 9 μL Cys with different concentrations was added. The results were recorded at 2 min by Huawei 5s camera. The calibration plot is shown in Fig. 3, and the inset is the corresponding photographs. The ΔRed/Blue ratio (excluding blank value) was proportional to the concentration of Cys. The calibration function was $y = 0.1652x + 0.0761$, and the linear correlation coefficient (R) was 0.9984. The results indicate that ΔRed/Blue is linear with the concentration of Cys over the range of 99.9–998.7 μM with a LOD of 1.0 μM. In experiments, it is found that when the average Red/Blue ratio (0.7425) is greater than the blank value (0.7410) by 0.0015, the color difference between them is visible. Therefore, the Cys concentration in this case (1.0 μM) was defined as the LOD. In order to evaluate the validity of the calibration plot, a simple comparison of the experimental and theoretical Cys concentrations based on the calibration plot was conducted (Table 2). The recovery was determined as reported previously [37]. The results show that the recovery was between 98.8% and 102.0%. It reveals the accuracy of the method.

Selectivity and the repeatability of the method

The selectivity of the Cys assay method was investigated. As shown in Fig. 4, compared with the remarkable color intensity ratio of Cys, the ratios show no obvious responses of several other amino acids. The selectivity of the method was further evaluated by comparing the results in the absence and presence of coexistent interfering ions and molecules. Equal amount of ions or molecules were added to the Cys sample (0.50 mM), and the Red/Blue ratio was recorded and analyzed (Table 3). The results show that equal amounts of Zn^{2+}, glucose, SO_3^{2-}, and vitamin C, et al. have no interference in the determination of Cys. All substances had a deviation in the range of $-3 \sim +3\%$. It reveals that the coexistent substances will not interfere with the Cys determination.

The repeatability of the method was also discussed. The relative standard deviation (RSD) of intra-day ($n = 5$) and inter-day ($n = 5$) was all smaller than 2% for Cys

Table 3 Effects of coexistence interfering substances on the reliability of test results

Substances	Glucose	Zn^{2+}	SO_3^{2-}	Vitamin C	Hcy	GSH	Phe	Ser	Trp	Val	Tyr
Cys	0.9420										
Cys + substances	0.9211	0.9338	0.9235	0.9377	0.9476	0.9533	0.9406	0.9431	0.9435	0.9328	0.9413
Deviation/%	−2.2	−0.3	−2.0	−0.4	0.6	1.2	−0.2	0.1	0.2	−1.0	−0.1

Table 4 Repeatability of Cys detection in intra-day and inter-day

Cys sample/mM	Inter-day ($n = 5$)			Intra-day ($n = 5$)		
	Red/Blue	Average	RSD/%	Red/Blue	Average	RSD/%
0.25	0.8682	0.8683	1.02	0.8788	0.8722	0.71
	0.8738			0.8667		
	0.8682			0.8708		
	0.8774			0.8660		
	0.8541			0.8786		
0.50	0.8914	0.8953	0.50	0.9024	0.9405	1.27
	0.8942			0.9132		
	0.8931			0.9193		
	0.8948			0.8931		
	0.9029			0.8945		
0.75	0.9463	0.9427	0.54	0.9409	0.9400	0.59
	0.9484			0.9358		
	0.9357			0.9374		
	0.9396			0.9364		
	0.9437			0.9493		

samples with different concentrations (Table 4). It reveals that the method has good repeatability. The better RSD which is attributed to the average color intensity of one image is used [37].

Determination of Cys in real samples

In order to show the potentiality of the method, the human plasma was chosen as sample. And to confirm the reliability of the data, sample recovery tests were conducted. As shown in Table 5, Cys concentration was (0.27 ± 0.02 mM) and the recoveries was from 99.2 to 101.1%. The satisfactory recoveries reveal the good validity of the method. The results prove that the method can be used to determine Cys in real sample. There were no severe interferences in these samples for Cys determination. According to the linear range of the calibration plot, pre-concentration is needed for urine samples because of its lower concentration [36].

Conclusion

Through amino groups, Asp modified AuNPs were synthesized. The colorimetric quantitation of Cys was obtained on the surface of a small paper patch (i.e., 6 mm) using the Asp-AuNPs. The method allows the Cys determination in the absence of UV-visible or fluorescence spectrophotometer. Its determined principle was the aggregation of Asp-AuNPs in the presence of Cys. With the aggregation, the color of Asp-AuNPs will change from red to blue. The results were recorded by a cell phone. The color intensity was analyzed by the Adobe Photoshop software. The ratio of color intensity value at red and blue channel (Red/Blue) increases with Cys concentration linearly. The assay method has the advantages of paper-based analytical devices and AuNPs. It shows good selectivity, portability, low cost, and etc.

Table 5 Determination of Cys in human plasma sample

Plasma sample	Red/Blue	Cys concentration/mM	Added Cys/mM	Found Cys/mM	Recovery/%
1#	0.9554	0.2906	0.1450	0.4345	99.2
2#	0.9560	0.2942	0.1450	0.4404	100.8
3#	0.9489	0.2512	0.1450	0.3953	99.4
4#	0.9505	0.2609	0.1800	0.4387	98.8
5#	0.9498	0.2567	0.1800	0.4387	101.1

Compliance with ethical standards

Conflict of interest The authors declare that they have no conflict of interest.

References

1. Weerapana E, Wang C, Simon GM, Richter F, Khare S, Dillon MBD, Bachovchin DA, Mowen K, Baker D, Cravatt BF (2010) Quantitative reactivity profiling predicts functional cysteines in proteomes. Nature 468:790–795

2. Zhou Y, Yoon J (2012) Recent progress in fluorescent and colorimetric chemosensors for detection of amino acids. Chem Soc Rev 41:52–67

3. Fu ZH, Han X, Shao Y, Fang J, Zhang ZH, Wang YW, Peng Y (2017) Fluorescein-based chromogenic and ratiometric fluorescence probe for highly selective detection of cysteine and its application in bioimaging. Anal Chem 89:1937–1944

4. Shahrokhian S (2001) Lead Phthalocyanine as a selective carrier for preparation of a cysteine-selective electrode. Anal Chem 73:5972–5978

5. EI-Khairy L, Ueland PM, Refsum H, Graham IM, Vollset SE (2001) Plasma total cysteine as a risk factor for vascular disease. Circulation 103:2544–2549

6. Wang XF, Cynader MS (2001) Pyruvate released by astrocytes protects neurons from copper-catalyzed cysteine neurotoxicity. J Neurosci 21:3322–3331

7. Nolin TD, McMenamin ME, Himmelfarb J (2007) Simultaneous determination of total homocysteine, cysteine, cysteinylglycine, and glutathione in human plasma by high-performance liquid chromatography: application to studies of oxidative stress. J Chromatogr B 852:554–561

8. Kang SH, Wei W, Yeung ES (2000) On-column derivatization for the analysis of homocysteine and other thiols by capillary electrophoresis with laser-induced fluorescence detection. J Chromatogr B 744:149–156

9. Rajaram R, Mathiyarasu J (2018) An electrochemical sensor for homocysteine detection using gold nanoparticle incorporated reduced graphene oxide. Colloids Surf B: Biointerfaces 170:109–114

10. Jun ME, Roy B, Ahn KH (2011) "Turn-on" fluorescent sensing with "reactive" probes. Chem Commun 47:7583–7601

11. Li Q, Liu F, Lu C, Lin J-M (2011) Aminothiols sensing based on fluorosurfactant-mediated triangular gold nanoparticle-catalyzed luminol chemiluminescence. J Phys Chem C 115:10964–10970

12. Chow C-F, Lam MHW, Leung MKP (2002) Fluorescent sensing of homocysteine by molecular imprinting. Anal Chim Acta 466:17–30

13. Zhang S, Wu D, Wu J, Xia Q, Jia X, Song X, Zeng L, Yuan Y (2019) A water-soluble near-infrared fluorescent probe for sensitive and selective detection of cysteine. Talanta 204:747–752

14. Cheng T, Huang W, Gao D, Yang Z, Zhang C, Zhang H, Zhang J, Li H, Yang X (2019) Michael Addition/S,N-intramolecular rearrangement sequence enables selective fluorescence detection of cysteine and homocysteine. Anal Chem 91:10894–10900

15. Cao N, Zhou H, Tan H, Qi R, Chen J, Zhang S, Xu J (2019) Turn-on fluorescence detection of cysteine with glutathione protected silver nanoclusters. Methods Appl Fluoresc 7:034004

16. Zhu M, Wang L, Wu X, Na R, Wang Y, Li QX, Hammock BD (2019) A novel and simple imidazo[1,2-a]pyridin fluorescent probe for the sensitive and selective imaging of cysteine in living cells and zebrafish. Anal Chim Acta 1058:155–165

17. Ning Z, Wu S, Liu G, Ji Y, Jia L, Niu X, Ma R, Zhang Y, Xing G (2019) Water-soluble AIE-active fluorescent organic nanoparticles: design, preparation and application for specific detection of cysteine over homocysteine and glutathione in living cells. Chem Asian J 14:2220–2224

18. Wang J, Lin X, Su L, Yin J, Shu T, Zhang X (2018) Chemical etching of pH-sensitive aggregation-induced emission-active gold nanoclusters for ultra-sensitive detection of cysteine. Nanoscale 11:294–300

19. Liu W, Kou J, Xing H, Li B (2014) Paper-based chromatographic chemiluminescence chip for the detection of dichlorvos in vegetables. Biosens Bioelectron 52:76–81

20. Li B, Zhang Z, Qi J, Zhou N, Qin S, Choo J, Chen L (2017) Quantum dot-based molecularly imprinted polymers on three-dimensional origami paper microfluidic chip for fluorescence detection of phycocyanin. ACS Sensors 2:243–250

21. Zhang H, Qiu X, Zou Y, Ye Y, Qi C, Zou L, Yang X, Yang K, Zhu Y, Yang Y, Zhou Y, Luo Y (2017) A dye-assisted paper-based point-of-care assay for fast and reliable blood grouping. Sci Transl Med 9:1–11

22. Xia Y, Si J, Li Z (2016) Fabrication techniques for microfluidic paper-based analytical devicesand their applications for biological testing: a review. Biosens Bioelectron 77:774–789

23. Choleva TG, Kappi FA, Giokas DL, Vlessidis AG (2015) Paper-based assay of antioxidant activity using analyte-mediatedon-paper nucleation of gold nanoparticles as colorimetric probes. Anal Chim Acta 860:61–69

24. Liu MM, Lian X, Liu H, Guo ZZ, Huang HH, Lei Y, Peng HP, Chen W, Lin XH, Liu AL, Xia XH (2019) A colorimetric assay for sensitive detection of hydrogen peroxide and glucose in microfluidic paper-based analytical devices integrated with starch-iodide-gelatin system. Talanta 200:511–517

25. Anand K, Abhiram H, Ravi KA, Monosree C, Kuldeep M, Keya L, Nripen C (2015) A paper based microfluidic device for easy detection of uric acid using positively charged gold nanoparticles. Analyst 140:7062–7081

26. Zhang H, Smith E, Zhang W, Zhou (2019) Inkjet printed microfluidic paper-based analytical device (μPAD) for glucose colorimetric detection in artificial urine. Biomed Microdevices 21:48. https://doi.org/10.1007/s10544-019-0388-7

27. Hamedpour V, Postma GJ, van den Heuvel E, Jansen JJ, Suzuki K, Citterio D (2018) Chemometrics-assisted microfluidic paper-based analytical device for the determination of uric acid by silver nanoparticle plasmon resonance. Anal Bioanal Chem 410:2305–2313

28. Rossini EL, Milani MI, Carrilho E, Pezza L, Pezza HR (2018) Simultaneous determination of renal function biomarkers in urine using a validated paper-based microfluidic analytical device. Anal Chim Acta 997:16–23

29. Qian Q, Deng J, Wang D, Yang L, Yu P, Mao L (2012) Aspartic acid-promoted highly selective and sensitive colorimetric sensing of cysteine in rat brain. Anal Chem 84:9579–9584

30. Liu L, Zhu G, Zeng W, Yi Y, Lv B, Qian J, Zhang D (2019) Silicon quantum dot-coated onto gold nanoparticles as an optical probe for colorimetric and fluorometric determination of cysteine. Microchim Acta 186(2):98

31. Pang B, Zheng Y, Wang J, Liu Y, Song X, Li J, Yao S, Fu K, Xu K, Zhao C, Li J (2019) Colorimetric detection of Staphylococcus aureus using gold nanorods labeled with yolk immunoglobulin and urease, magnetic beads, and a phenolphthalein impregnated test paper. Microchim Acta 186(9):611

32. Raj DR, Sudarsanakumar C (2018) Colorimetric and fiber optic sensing of cysteine using green synthesized gold nanoparticles. Plasmonics 13(1):327–334

33. Jeyasekaran E, Venkatachalam S (2019) Colorimetric detection of cysteine based on dispersion-aggregation mechanism of chitosan stabilized gold nanoparticles. Can J Chem 197(3):233–237

34. Chen Z, Luo S, Liu C, Cai Q (2009) Simple and sensitive colorimetric detection of cysteine based on ssDNA-stabilized gold. Anal Bioanal Chem 395(2):489–494

35. Li W, Zhi X, Yang J, Zhang J, Fu Y (2016) Colorimetric detection of cysteine and homocysteine based on an oligonucleotide-stabilized Pd nanozyme. Anal Methods 8(25):5111–5116

36. Prasetia R, Fuangswasdi S, Unob F (2019) Silver nanoparticle-supported hydroxyapatite as a material for visual detection of urinary cysteine. Anal Methods 11(22):2888–2894

37. Liu C, Gomez FA, Miao Y, Cui P, Lee W (2019) A colorimetric assay system for dopamine using microfluidic paper-based analytical devices. Talanta 194:171–176

Publisher's note Springer Nature remains neutral with regard to jurisdictional claims in published maps and institutional affiliations.